

# An Investigation into Computational Modelling of Cavitation in a Propeller's Slipstream

Naz Yilmaz<sup>1</sup>, Mahdi Khorasanchi<sup>1</sup>, Mehmet Atlar<sup>1</sup>

<sup>1</sup>University of Strathclyde, Glasgow, United Kingdom

## ABSTRACT

This paper reports on the ongoing developments of cavitation modelling so far which include preliminary validation studies for simulating the performances of two benchmark model propellers: i.e. PPTC propeller with inclined shaft; and E779A propeller, in non-cavitating and cavitating conditions. The main purpose of this study is to estimate the propeller's performance in cavitating conditions particularly developing tip vortex cavitation. The simulations in open water and cavitating conditions were carried out in uniform flow using a commercial CFD package. Firstly, the validation studies were conducted for non-cavitating condition. The comparison with the benchmark experimental data showed good agreement for the thrust and torque coefficients as well as for the open water efficiency. Next, the cavitation developed on the propeller was simulated using a numerical model based on the Rayleigh-Plesset equation. Propulsion coefficients ( $K_T$ ,  $K_Q$ ) and the cavity patterns on the benchmark propellers' blades showed very good agreement with the experimental data. However, the tip vortices off the blades could only be traced for E779A propeller by using a new mesh refinement approach.

## Keywords

Marine Propellers, Tip Vortex Cavitation, CFD, RANS, DES.

## 1 INTRODUCTION

Computational modelling of a tip and hub vortex cavitation in a propeller's slipstream is a real challenge for CFD users. Although prediction of cavitation on the propeller blade surfaces has been tackled by many researchers, the efforts for stretching the model to include the tip vortex and hub cavitation leaving the propeller and reaching rudder are rather scarce.

The results of Rome Workshop on E779A propeller including cavitation were presented by Salvatore et al. (2009). Different computational models i.e. RANS, LES and BEM were compared in non-cavitating and cavitating conditions for the propeller performance including pressure distributions and cavitation patterns on the blades.

Many researchers have reported on their predictions for the hydrodynamic behaviour of the PPTC propeller test

cases with and without shaft inclination. For example, Guilmineau et al. (2015) investigated this benchmark propeller with inclined shaft in cavitating and non-cavitating conditions using  $k-\omega$  SST model in solver ISIS-CFD. Pressure distribution and cavitation pattern on blade surfaces were evaluated as well as propeller performance characteristics. Lloyd et al. (2015) reported the results of the same case with various mesh density (course, medium and fine) for both open water and cavitating conditions in terms of pressure pulses and cavitation pattern using CFD code ReFRESCO. Morgut and Nobile (2012) studied cavitation of PPTC and E779A propellers in a uniform flow using Ansys CFX software. Three different mass transfer models, i.e. Kunz, Zwart and FCM (Full Cavitation Model) were implemented.

The above mentioned studies showed good agreement with experiments for the propeller performance characteristics, pressure distribution and cavitation pattern on the blade surfaces, however tracing tip vortex and hub cavitation in the slipstream has been still a challenge for researchers.

To this end, Fujiyama et al. (2011) created a fine mesh region around tip area of PPTC propeller with level shaft to capture tip vortex cavitation using RANS model and SC/Tetra CFD software. With this mesh refinement, the cavitation pattern was simulated on blade surfaces and moreover a small extension of tip vortex cavitation was observed.

Despite the major improvements in numerical analysis of propeller performance, modelling tip vortex and hub cavitation is not yet satisfactory to estimate the propeller performance in cavitating conditions accurately. This study is therefore an attempt to improve tip vortex cavitation model using a new mesh approach.

## 2 NUMERICAL METHOD

In this paper, PPTC (with shaft inclination) and E779A propellers were investigated in open water and cavitating conditions using Star CCM+ software. Ansys Fluent was also used for one of the cases of E779A propeller in non-cavitating conditions for comparison. RANS (Reynold-Averaged Navier Stokes) model with  $k-\omega$  SST turbulence model and DES (Detached Eddy Simulations) were preferred for this study. A detailed numerical treatment of

RANS model was presented by Ferziger & Peric (1996) and Wilcox (1994). DES model was well described by Spalart et al. (1997) and Spalart (2009).

For modelling multiphase flow of water and vapour, VOF (Volume of Fluid) method was adopted. Schneer-Sauer cavitation model (Schneer and Sauer 2001) which is based on reduced Rayleigh-Plesset equation (Plesset, 1977) was implemented. Although the cavitation is influenced by many parameters such as velocity, density, viscosity, saturation and static pressures, surface tension and so on, this method in contrast to Full Rayleigh-Plesset model neglects the influence of bubble growth acceleration, surface tension as well as viscous effects between water and vapour phases (Star CCM+ User Guide, 2016).

The cavitation number based on rotational speed of the propeller is defined as

$$\sigma_n = \frac{p - p_{sat}}{0.5\rho_l(nD)^2} \quad (1)$$

Where  $p$  is the tunnel pressure,  $p_{sat}$  is the vapour pressure,  $\rho_l$  is the density of the fluid,  $n$  is the rotation rate and  $D$  is the diameter of the propeller.

The advance ratio is defined as

$$J = \frac{V_A}{nD} \quad (2)$$

Where  $V_A$  is the advance velocity of fluid. Thrust and torque coefficient of the propeller is calculated as

$$K_T = \frac{T}{\rho n^2 D^4} \quad (3)$$

$$K_Q = \frac{Q}{\rho n^2 D^5} \quad (4)$$

Where  $T$  and  $Q$  are thrust and torque values of the propeller respectively and  $\rho$  is density of fluid. The open water efficiency of propeller is defined as below.

$$\eta_0 = \frac{J K_T}{2\pi K_Q} \quad (5)$$

### 3 MODEL SCALE PROPELLERS

The PPTC (Postdam Propeller Test Case) and E779A propellers were chosen as a benchmark for the validation study.

The PPTC propeller is a five-bladed, right handed CPP (Controllable Pitch Propeller) fitted on an open water test rig set with 12 degrees shaft inclination and was used as a test case for The SMP'15 Propeller Workshop in 2015. The experimental data in this workshop was provided by SVA (Postdam Model Basin) test facility. The same propeller was tested at level (zero) shaft inclination and associated results were used in The SMP'11 Propeller Workshop in 2011. The experimental data of both workshops including open water tests, cavitation tests and pressure pulses results have been used by many researchers for validation studies.

The E779A propeller is a four-bladed, low skew FPP (Fixed Pitch Propeller) fitted on an open water test rig

with zero shaft inclination and was designed in 1959. This propeller was tested by INSEAN (Istituto Nazionale di Studi ed Esperienze di Architettura Navale) in non-cavitating and cavitating conditions.

Figure 1 and Table 1 demonstrate the geometries and main particulars of PPTC and E779A propellers respectively.

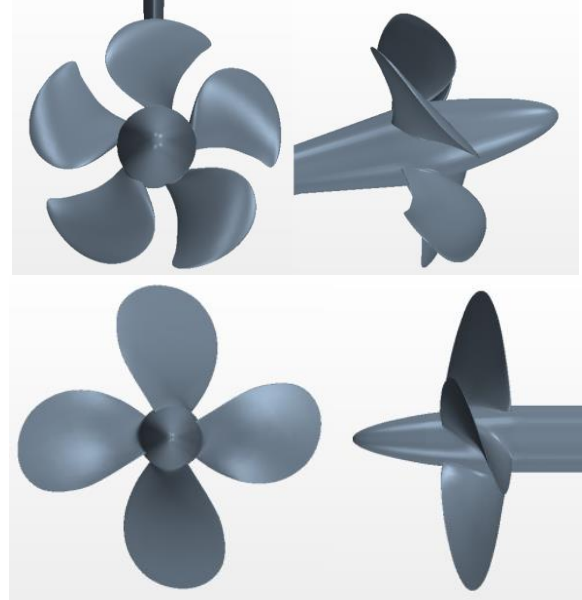


**Figure 1. CAD geometries of the benchmark propellers (Top: PPTC propeller with inclined shaft. Bottom: E779A Propeller with horizontal shaft)**

**Table 1. Particulars of the Propellers**

Propeller	PPTC	E779A
Number of Blades (Z)	5	4
Diameter (D)	0.250m	0.227m
Pitch Ratio (P/D)	1.6	1.1
Area Ratio ( $A_E/A_0$ )	0.78	0.69

### 4 SIMULATION OF NON-CAVITATING CASE

The validation studies were conducted using both propellers in non-cavitating open water conditions. For detailed experimental results, refer to Salvatore et al. (2009) for E779A propeller and Postdam Evaluation Reports Case 1 (2015) for PPTC propeller with shaft inclination.

The simulations of PPTC propeller were carried out at five different flow speeds using k- $\omega$  SST turbulence model and sliding mesh technique for describing the rotation. The analyses were conducted with the five blades of the propeller and using two computational domains, i.e. rotating and stationary domains. Table 2 demonstrates CFD and EFD (Experimental Fluid Dynamics) results and the differences between these results at five advance ratios. Although the difference was 1% at  $J=1$ , this increased to 8% for  $J=1.4$ .

The similar validation study was also carried out for the E779A propeller at only one flow speed using two

different software packages i.e. Ansys Fluent and Star CCM+. In the former case, one rotating domain was prepared with an unstructured mesh of 1.7M cells and MRF (Moving Reference Frame) technique was adapted to model propeller rotation. In contrast, sliding mesh technique was used in Star CCM+ with two domains and a structured mesh of 3.2M cells. Figure 2 shows unstructured and structured meshes generated by Ansys Fluent and Star CCM+ respectively.

The comparison of results from two CFD solvers showed a good agreement with experiment for the thrust and torque coefficients as well as the open water efficiency (Table 3).

### 5 SIMULATION OF CAVITATING CASE

The same test case was used to estimate the hydrodynamic performances of the propellers in cavitating conditions using Star CCM+. A new refined grid was generated for each propeller to capture the bubbles. The cavitation simulations were carried out using Schneer-Sauer cavitation model that is based on Rayleigh-Plesset equation (Plesset, 1977).

#### 5.1 Computational Domain

A similar domain dimensions as provided in Propeller Workshop SMP'15 was used for PPTC propeller. That is approximately 1.5D, 8D and 2D from the centre of propeller to sides, outlet and inlet respectively. This domain geometry includes propeller, shaft and bracket.

For E779A propeller, the distance of the propeller centre in axial direction from the inlet and outlet of the computational domain was 5D and 13D respectively according to recommendation of Star CCM+ user guide (Star CCM+ User Guide, 2016). Figure 3 shows the geometry of the computational domains and boundary conditions.

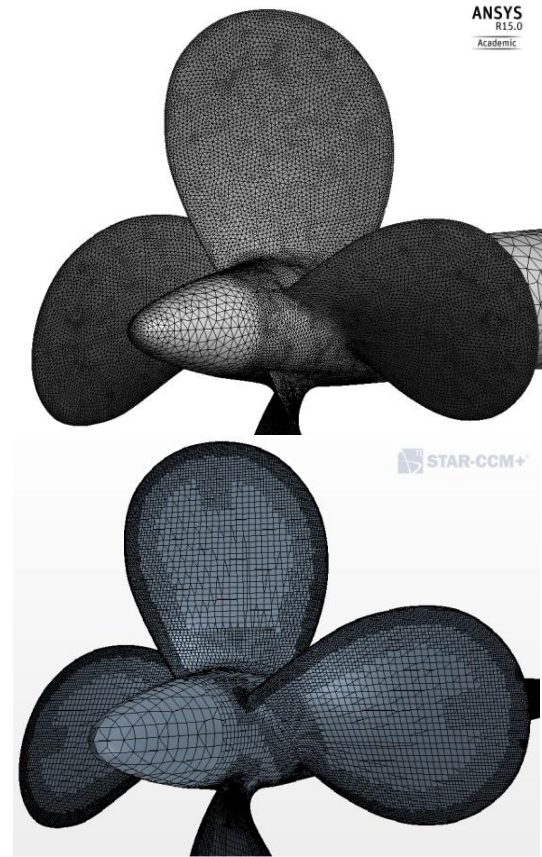


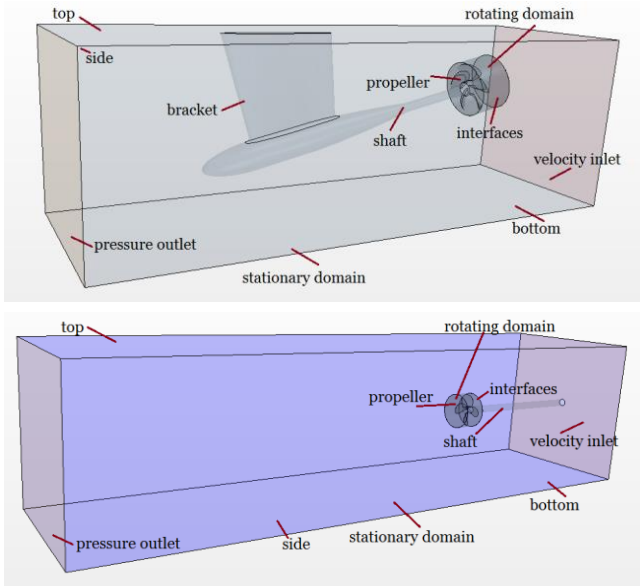
Figure 2. Grid generation of open water simulations for E779A propeller (Top: Unstructured mesh in Ansys Fluent, Bottom: Structured mesh in Star CCM+)

Table 2. Open water comparison between CFD and EFD results for PPTC propeller

Case	CFD Results			EFD Results			Difference (CFD & EFD)		
	$K_T$	$10K_Q$	$\eta_0$	$K_T$	$10K_Q$	$\eta_0$	$K_T$	$10K_Q$	$\eta_0$
0.6	0.654	1.463	0.426	0.621	1.425	0.416	5%	3%	3%
0.8	0.531	1.248	0.542	0.509	1.215	0.533	4%	3%	2%
1.0	0.409	1.028	0.633	0.404	1.023	0.628	1%	1%	1%
1.2	0.294	0.813	0.692	0.303	0.838	0.691	-3%	-3%	0%
1.4	0.182	0.585	0.694	0.198	0.636	0.695	-8%	-8%	0%

Table 3. Open water comparison between CFD and EFD results for E779A propeller

Software	Case	Performance Coefficient			Difference (CFD & EFD)		
		$K_T$	$10K_Q$	$\eta_0$	$K_T$	$10K_Q$	$\eta_0$
Ansys Fluent	0.71	0.222	0.419	0.600	-6%	-2%	-4%
Star CCM+	0.71	0.229	0.428	0.606	-3%	0%	-3%
EFD Results	0.71	0.238	0.429	0.626	-	-	-



**Figure 3. Computational domain and boundary conditions (Top: PPTC propeller with inclined shaft, Bottom: E779A propeller)**

### 5.2 Grid Generation and Conditions

A suitable new mesh was generated for each propeller case with smaller surface size ( $0.002D$ ) on the blade surfaces than the generated mesh previously for the open water case. Figure 4 demonstrates the grid for both propellers. The finer meshes were generated for the cavitation cases with approximately 6 and 14 million cells for PPTC and E779A propellers respectively. Although the similar grid sizes were used on the blade surfaces, the difference between two meshes is due to different domain size and volumetric control geometries. The average  $y^+$  value (Figure 5) was around 1 and less for blades and shaft respectively of E776A propeller using 12 prism layers and approximately 1 mm total thickness. Three cases, in terms of  $J$  values and cavitation numbers, were analysed for PPTC propeller with inclined shaft. RANS method with  $k-\omega$  SST turbulence model and DES method were used and a small improvement on cavitation pattern

was observed with DES method. Thus, the cavitation simulations were carried out for E779A propeller using DES method for two different cases in term of  $J$  and cavitation number values. The model settings of each case study are given in Tables 4 and 5. The case descriptions were obtained from the reports of the SMP'15 Propeller Workshop for PPTC and from literature for E779A propeller (Pereira et al. 2004, Salvatore et al. 2009).

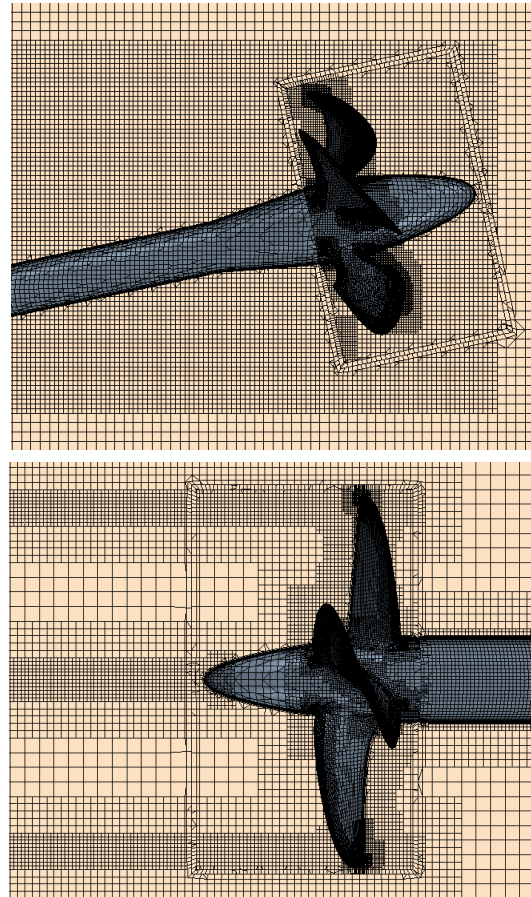


**Figure 4. Computational Grid (Top; PPTC propeller with inclined shaft, Bottom; E779A propeller)**

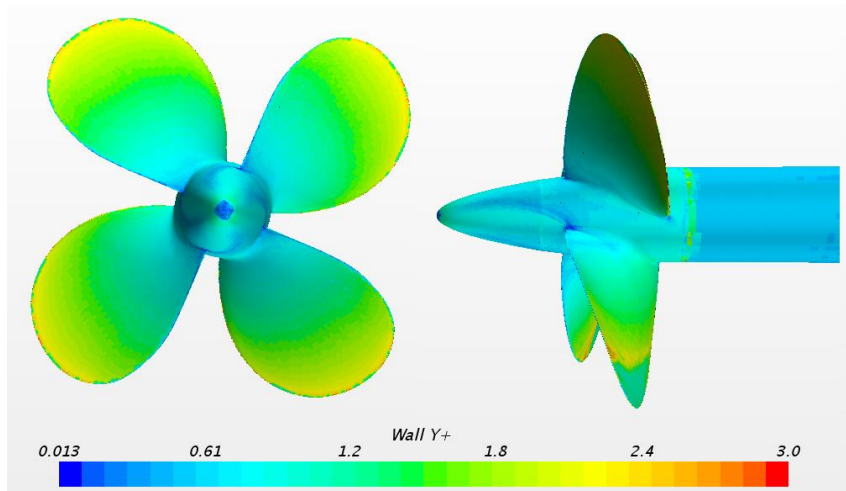


**Figure 5.  $y^+$  on blades, hub and shaft for E779A propeller**

**Table 4. Model Settings for PPTC propeller**

Variables	Symbol	Cases			Unit
		Case 2.1	Case 2.2	Case 2.3	
Advance Coefficient	J	1.019	1.269	1.408	[]
Cavitation Number based on n	$\sigma_n$	2.024	1.424	2.000	[]
Number of Revolutions	n	20	20	20	[1/s]
Water Density	$\rho$	997.78	997.78	997.41	[kg/m <sup>3</sup> ]
Kinematic Viscosity of Water	$\nu$	$9.567 \cdot 10^{-7}$	$9.591 \cdot 10^{-7}$	$9.229 \cdot 10^{-7}$	[m <sup>2</sup> /s]
Vapour Pressure	$P_v$	2643	2626	2904	[Pa]

**Table 5. Model Settings for E779A propeller**

Variables	Symbol	Cases		Units
		Case 1	Case 2	
Advance Coefficient	J	0.71	0.77	[]
Cavitation Number based on n	$\sigma_n$	1.763	2.082	[]
Vapour Pressure	$P_v$	3170.34	2338	[Pa]

### 5.3 Results

A comparison of simulation results with experimental data of PPTC propeller (Postdam Evaluation Reports Case 2, 2015) is presented in Table 6 and cavitation pattern is compared in Figures 6 and 7. Although the results of Case 2.1 showed good agreement, there existed some discrepancies in propeller performance coefficients between CFD and EFD in Case 2.2 and Case 2.3 of PPTC propeller. Similar range of deviation was reported for  $K_T$  by other researchers in previous workshop, varying from 7%, 24% and 18% for Case 2.1, 2.2 and 2.3 respectively (Postdam Evaluation Reports Case 2, 2015). Nevertheless, the cavitation pattern on blade surface showed very good agreement although tip vortex cavitation extent could not be simulated with these mesh and settings.

Despite the fine mesh and DES model, the cavitation pattern was only observed on E779A blade surfaces and hub (Figure 8) with a good agreement with experiments (Pereira et al. 2004, Salvatore et al. 2009). Though it was concluded this mesh and analysis method were not sufficient to capture the tip vortex cavitation.

**Table 6. Comparison between CFD and EFD, PPTC propeller**

		Case 2.1	Case 2.2	Case 2.3
$K_T$	CFD	0.393	0.214	0.149
	EFD	0.363	0.167	0.123
	Difference	9%	28%	21%

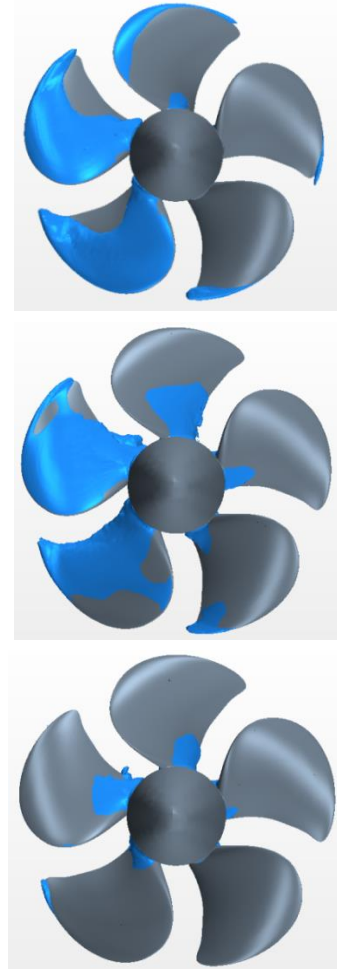


**Figure 6. Cavitation pattern on PPTC blade, suction side (VOF of vapour; 50%) (From top to bottom; Case2.1, Case2.2 and Case2.3)**

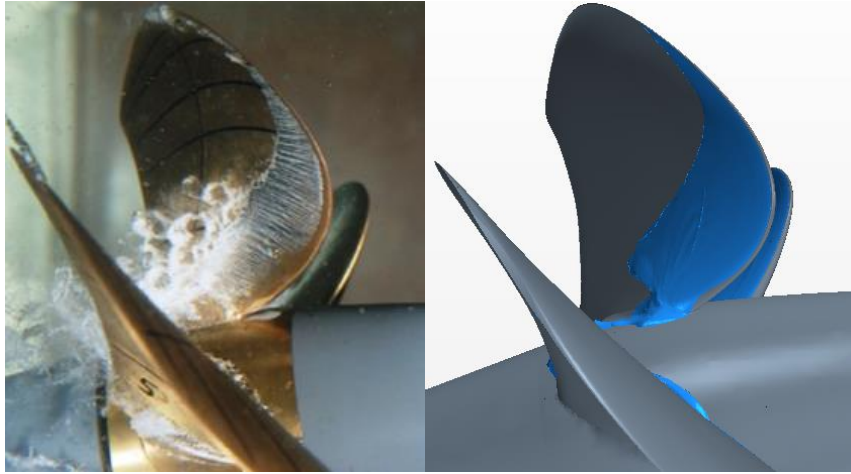


Figure 7. Comparison between EFD and CFD, PPTC propeller (VOF of vapour; 50%) (Case 2.3)

Table 7. CFD and EFD results for E779A propeller in cavitating conditions

	Case	Performance Coefficient			Difference		
		J	$K_T$	$10K_Q$	$\eta_0$	$K_T$	$10K_Q$
CFD (RANS)	0.71	0.234	0.434	0.609	-8%	-6%	-3%
CFD (DES)	0.71	0.234	0.436	0.607	-8%	-5%	-3%
EFD	0.71	0.255	0.460	0.626	-	-	-

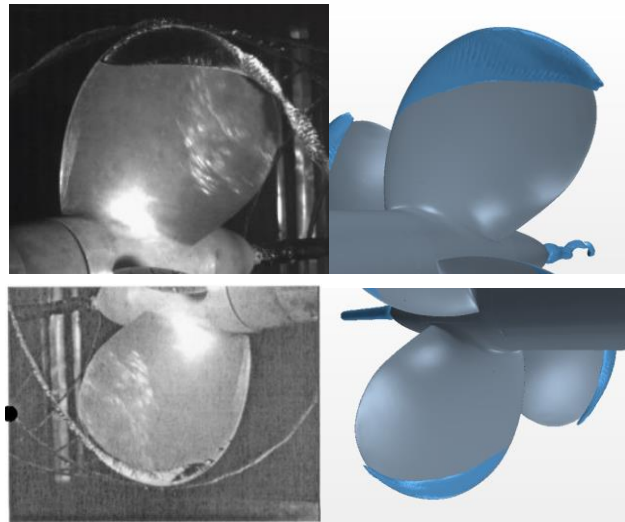


Figure 8. Comparisons between EFD and CFD, E779A propeller (Top; Case 1;  $J=0.71$ ,  $\sigma_n=1.763$ , Bottom; Case 2;  $J=0.77$ ,  $\sigma_n=2.082$ )

### 6 TIP VORTEX CAVITATION

The above validation studies indicated that the simulation method has to be improved to tip vortex and hub cavitation using different solver models as well as the type, surface size and refinement of the mesh. For this reason, a helical tube around the propellers' tip (Figure 9) was created for further mesh refinement. The main purpose of this application is to create a very fine mesh around tip area where the tip vortex cavitation probably occurs (Figure 10). The simulation was repeated with approximately 11 million cells. The average  $y^+$  value was

kept the same as the prism layer settings were not changed in the new mesh.

In addition to the helical tube geometry, cylinder geometry was prepared to create a volumetric control for capturing the extension of hub cavitation as well (Figure 10). These techniques made an extension of the tip vortex and hub cavitation appears (Figures 11). The cavitation pattern was compared with experiment in Figure 12. It was observed that the improvement of the tip vortex cavitation is directly related to the mesh refinement. In this case, the mesh size in the volumetric control around

tip was selected as  $0.001D$  after a few iterations. After creating the helical tube geometry and using it for the mesh refinement, extension of the tip vortex could featly be simulated. Moreover, the thrust and torque coefficients were dropped due to cavitation impact (Table 8).

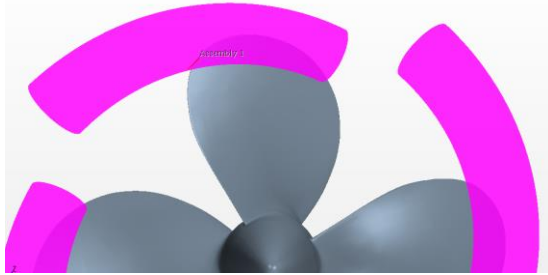


Figure 9. Helical tube around propeller's tip

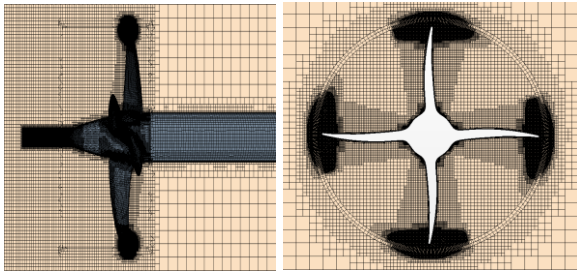


Figure 10. Grid Generation with refinement using the helical tube geometry

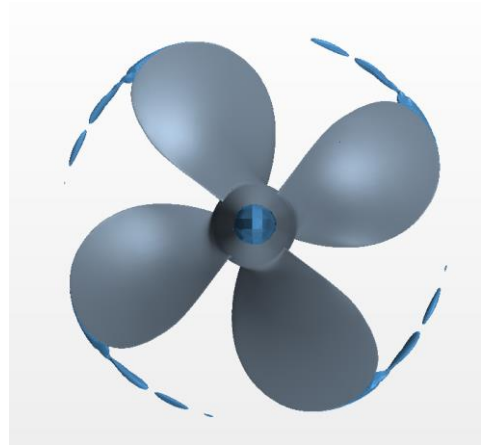
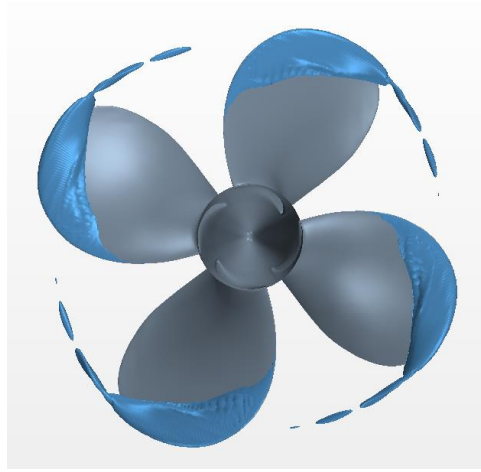


Figure 11. Cavitation Pattern on blade surface and tip vortex cavitation (VOF of vapour; 50%) (Top; Suction side, Bottom; Pressure Side)

Table 8. CFD and EFD results for E779A propeller in cavitating conditions with and without tip vortex refinement

Tip Vortex Refinement	Case	Performance Coefficient			Difference		
		$K_T$	$10K_Q$	$\eta_0$	$K_T$	$10K_Q$	$\eta_0$
With	0.71	0.230	0.432	0.601	-10%	-6%	-4%
Without	0.71	0.234	0.436	0.607	-8%	-5%	-3%
EFD	0.71	0.255	0.460	0.626	-	-	-

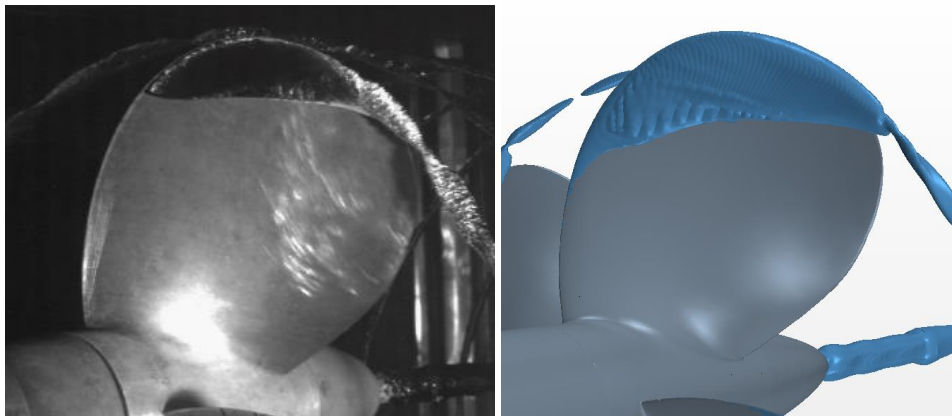


Figure 12. Comparison between EFD and CFD, tip vortex and hub cavitation (VOF of vapour; 50%)

## 7 CONCLUSIONS AND FUTURE WORKS

This study was an attempt to improve computational modelling of tip vortex cavitation in marine propellers. First, the cavitation pattern on blade surface was simulated and validated against the experimental results. Though, it was concluded that the current approach was not sufficient to determine the propeller performance in cavitating conditions accurately. Next, a special mesh refinement showed that the mesh size especially in the area where the cavitation probably occurs must be fine enough to capture the tip vortex cavitation. An extension of mesh refinement area may further improve simulation of tip vortex cavitation however results in more computational cost. This improvement will be used for investigation of the propeller and rudder interaction in future.

## 8 ACKNOWLEDGEMENTS

The first author was sponsored by Turkish Ministry of Education during this study. The authors are also thankful for granted access to High Performance Computing for the West of Scotland (Archie-West). They are also grateful to INSEAN, especially Francesco Salvatore, for providing the geometry of E779A propeller and sharing the experimental results.

## 9 REFERENCES

- Carlton J. (2007). 'Marine Propellers and Propulsion'. Elsevier Ltd.
- Ferziger, J. H. & Peric, M. (1996). 'Computational Methods for Fluid Dynamics'. Springer-Verlag.
- Fujiyama, K., Kim, C. H., Hitomi, D. (2011). 'Performance and Cavitation Evaluation of Marine Propeller using Numerical Simulations'. Second International Symposium on Marine Propulsors smp'11, Hamburg, Germany.
- Guilmineau, E., Deng, G. B., Leroyer, A., Queutey, P., Visonneau, M., Wackers, J. (2015). 'Numerical Simulations of the Cavitating and Non-Cavitating Flow around the Postdam Propeller Test Case'. Fourth International Symposium on Marine Propulsors smp'15, Austin, Texas, USA.
- Lloyd, T., Guilherme, V., Rijpkema, D., Schuiling, B. (2015). 'The Postdam Propeller Test Case in oblique flow: prediction of propeller performance, cavitation patterns and pressure pulses'. Second International Workshop on Cavitating Propeller Performance, Austin, Texas, USA.
- Morgut, M. & Nobile, E. (2012). 'Numerical Predictions of Cavitating Flow around Model Scale Propellers by CFD and Advanced Model Calibration'. International Journal of Rotating Machinery, Volume 2012, Article ID 618180.
- Pereira, F., Salvatore, F., Felice, F. D., (2004). 'Measurement and Modeling of Propeller Cavitation in Uniform Inflow'. Journal of Fluids Engineering, Vol. 126.
- Plesset, M. S. & Prosperetti, A. (1977). 'Bubble Dynamics and Cavitation'. The Annual Review of Fluid Mechanics, Vol 9.
- Postdam evaluation reports (2015). 'Propeller Open Water Curves in Oblique Flow'. Fourth International Symposium on Marine Propulsors smp'15, Austin, Texas.
- Postdam Evaluation Reports Case 1 (2015). 'Propeller Open Water Curves in Oblique Flow'. Fourth International Symposium on Marine Propulsors smp'15, Austin, Texas.
- Postdam Evaluation Reports Case 2 (2015). 'Cavitation Test in Oblique Flow'. Fourth International Symposium on Marine Propulsors smp'15, Austin, Texas.
- Salvatore, F., Streckwall, H., Terwisga, T. (2009). 'Propeller Cavitation Modelling by CFD- Results from the VIRTUE 2008 Rome Workshop'. First International Symposium on Marine Propulsors smp'09, Trondheim, Norway.
- Schneer, G. H. & Sauer, J. (2001). 'Physical and Numerical Modelling of Unsteady Cavitation Dynamics'. International Conference on Multiphase Flow, New Orleans, USA.
- Spalart P. R. (2009). 'Detached-Eddy Simulation'. The Annual Review of Fluid Mechanics, 41.
- Spalart P. R., Jou, W.H., Strelets, M., Allmaras, S. R., (1997). 'Comments on the Feasibility of LES for Wings, and on a Hybrid RANS/LES Approach'. Advances in DNS/LES. Proceedings of the First AFOSR international Conference on DNS/LES, Louisiana Tech University, Ruston, Louisiana, USA.
- Star CCM+ User Guide, 2016
- Wilcox, D. C. (1994). 'Turbulence Modeling for CFD'. DCW Industries Inc. La Canada, California.